The 2009 IEEE/RSJ International Conference on
Intelligent Robots and Systems
October 11-15, 2009 St. Louis, USA

Real Time Motion Generation and Control for Biped Robot -3rd Report: Dynamics Error Compensation-

Toru Takenaka, Takashi Matsumoto and Takahide Yoshiike

***Abstract*—Trajectories generated from approximate dynamics models can lead biped robots to fall down due to the difference of dynamics between the approximate dynamics model and the real robot. In this paper, we propose real time methods to compensate for the dynamics error using dynamics error compensation models. Our methods satisfy the horizontal ground reaction force and moment limits so that no slip is caused with the ground. We also propose a method to compensate for the knee dynamics error which is not modeled in our approximate dynamics models. Combining these techniques, running motion is achieved on a real biped.**

I. Introduction

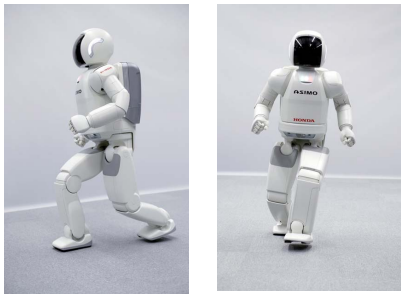

Fig. 1 Running biped robot system (ASIMO)

For biped robots [1][2] (Fig. 1) to exist around and collaborate with human, they need abilities to react robustly against unknown events including avoiding collision with previously unknown obstacles and maintaining balance under external disturbances by taking steps. Real time techniques to generate a variety of dynamically stable motions are required to achieve such behaviors.

Because of its high degrees of freedom, highly nonlinear dynamics and kinematic constraints, it is difficult to use detailed dynamics models of biped robots to generate their motions in real time. Thus, approximate dynamics models are widely used to generate motions in real time [3][4][5][6][7].

Due to the approximated dynamics, motions generated with approximate dynamics model cannot be followed exactly by the real robot. Yamane et al. [8] and Nagasaka [13] have proposed methods to minimize the dynamics error using optimization techniques. These approach require large computation time and cannot be used in real time.

Kajita et al. [9] proposed a method to compute the translational and rotational velocities of the upper body and free ends to achieve desired translational and angular momentum. Kajita et al. [7] also proposed predictive control techniques to compensate for the dynamics approximation error with a feedback loop. These approaches ignore friction limits of ground and the resulting motion can lead to a slip.

In this paper, we propose methods to compensate for the dynamics error while explicitly taking the horizontal ground reaction force limits into account. We use an inverted pendulum model and a flywheel model [14] to account for the dynamics error. Using these techniques, the dynamics error is compensated and the horizontal ground reaction force limits are satisfied simultaneously. In addition, we propose a method to kinematically account for the knee bending motion of the detailed robot model for the motion generated from an approximate dynamics model without knees. Using these techniques, fast motions such as walking and running generated from approximate dynamics models are realized on a real robot.

In section II, a general overview of the system is given. From section III to V, the approximation model of the robot dynamics and gait pattern modification using them are introduced. Experimental results are shown in section VI.

II. System Overview

In this paper, a gait pattern is a set of trajectories for the desired ZMP, the feet and the upper body.

Given a command to move, step position and duration are decided (Fig. 2(a)).

Given parameters above, design the desired ZMP and feet trajectories. Then design the upper body trajectory which enables the desired ZMP trajectory without causing the upper body to diverge (Fig. 2(b)).

Feed the gait pattern into the real robot, and stabilize it while it is following the gait pattern (Fig. 2(c)).

Walking and running gait generations are explained in [10] and [11] respectively, and the balance controller is explained in [12].

This paper addresses the dynamics error compensation (Fig. 2(e)) in detail. The dynamics error compensation consists of the knee dynamics compensation (Fig. 2(f)) and the dynamics error compensation with the ground reaction force limits (Fig. 2(g)).

Fundamental Research Center, Honda Research & Development, 8-1 Honcho, Wako-shi, Saitama, Japan.

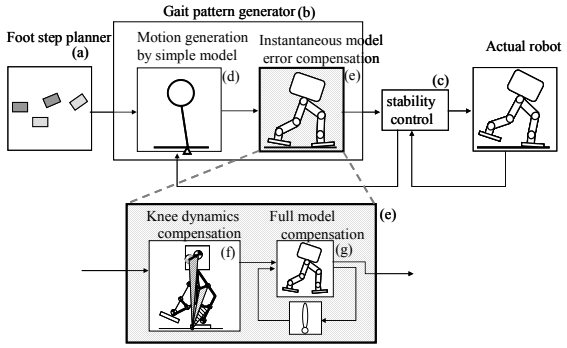

Fig. 2 System overview

III. Gait Pattern Modification with Dynamics Error Compensation Models

We design the desired ZMP trajectories with approximate dynamics models. If a detailed dynamics model tries to follow these trajectories, horizontal ground reaction moments are generated about the desired ZMP due to different dynamics. We measure this dynamics error as the horizontal ground reaction moment generated by the detailed dynamics model about the desired ZMP trajectory designed with the approximate models. This moment is zero if a trajectory generated from and followed by the same model, and thus we use it as a measure of dynamics error between two different dynamics models.

Instead of treating the dynamics difference directly, we use models representing the position and the angle of the upper body to cancel the horizontal ground reaction moment to 0. One of the advantages of this approach is that the kinematic constraints and redundancy of the detailed dynamics models can be ignored. Another advantage is computational efficiency which is critical to satisfy real time requirement. Redundancy of the legs of the detailed dynamics model is not discussed in this paper.

The dynamics error compensation models are an inverted pendulum and a flywheel (Fig. 3). In this paper, we limit our discussions to motions in saggital plane, but similar compensation is done in the lateral plane as well on a real robot.

The motion of the inverted pendulum model (Fig. 3(a)) is governed by the following dynamics equations.

$$m_{pend} h \ddot{x}_{pend} = m_{pend}(g + \ddot{z}_{pend}) * x_{pend} + M_{pend} \quad (1)$$

$$F_{pend} = m_{pend} \ddot{x}_{pend} \quad (2)$$

$$\Delta M_{pend} = h \Delta F_{pend} \quad (3)$$

where

x_{pend} : horizontal position of the pendulum.

m_{pend} : mass of the pendulum.

F_{pend} : ground reaction force of the pendulum.

M_{pend} : ground reaction moment of the pendulum.

$\ddot{z}_{pend}$: vertical acceleration of the pendulum.

h : height of the pendulum.

g : gravitational acceleration constant.

Even though the pendulum accelerates vertically, we assume the vertical motion is small enough and can be approximated by a constant. As implied in Eq. (3), the inverted pendulum requires the ground reaction force to generate the ground reaction moment.

The flywheel model (Fig. 3(b)) represents the motion of the robot in which moment is generated while the CoG stays still.

$$I \ddot{\theta}_{wheel} = M_{wheel} \quad (4)$$

where I is the characterized from the real robot.

On the real robot, inclining the upper body forward without translating it causes the CoG to move forward. To mimic the behavior of the flywheel, the upper body of the robot has to be shifted horizontally by x_{wheel} as follows so that the CoG of the robot does not move.

$$x_{wheel} = C \theta_{wheel} \quad (5)$$

where C is a constant identified from an upright posture of the real robot.

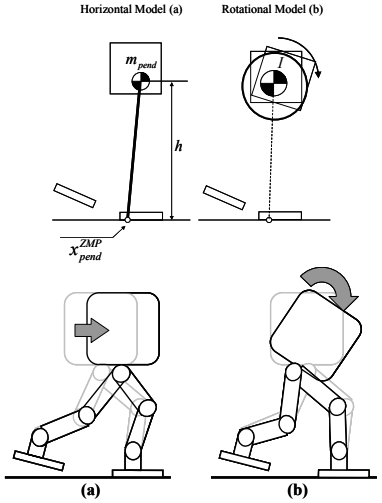

Fig. 3 Dynamics error compensation models

IV. Feedforward and Feedback Dynamics Compensation Methods

In this section, the following three feedforward (FF) methods and a feedback (FB) method to compensate for the dynamics error between approximate dynamics models and the real robot are explained.

1. FF compensation method which ignores ground reaction force limits
2. FF compensation method which satisfies ground reaction force limits.
3. FF compensation method which satisfies both ground reaction force limits and moment limits.

Only the third FF method is implemented in our system, but the other two FF methods are used for the ease of explaining.

A. Feedforward Dynamics Error Compensation without Ground Reaction Force Limits

Fig. 4 is the block diagram of the first compensation method which ignores the ground reaction force limits. This is equivalent to Kajita et al. [7] except that we do not use preview control.

The desired ZMP trajectory x_{zmp}, feet trajectory and upper body position x_{body_cmd} and inclination θ_{body_cmd} are designed using an approximate dynamics model. These are transformed into desired angle for each joint through inverse kinematics on the detailed dynamics model. Now, the moment about the desired ZMP, M_{full}, and the ground reaction force, F_{full} can be computed. M_{full} is caused due to the difference between the two dynamics models and thus ideally is 0. The goal of the dynamics compensation is to make M_{full} to 0 using the inverted pendulum model introduced earlier. This can be achieved by substituting $-M_{full}$ into M_{pend} in Eq. (1) and adding resulting x_{pend} into x_{body_cmd}. This usually causes the inverted pendulum to diverge. To prevent it, a stabilizing control which outputs M_{pend_stab} is enhanced to make x_{pend} 0. The stabilizing controller can be a simple PD controller for example. An example controller for running motion is introduced in [12]. The sum of requested dynamics compensation moment and pendulum stabilizing moment, $(-M_{full} + M_{pend\_stab})$, is then input to the pendulum, and the output x_{pend} is added to x_{body_cmd} to obtain the modified desired upper body position x_{body_mdfd}. M_{pend_stab} prevents the inverted pendulum from converging, however it also becomes the moment about the original desired trajectory. Thus, M_{pend_stab} becomes the ground reaction moment of modified gait pattern M_{mdfd}. The control scheme shown in Fig. 4 tries to make the difference of M_{full} and M_{mdfd} to 0. M_{mdfd} behaves like low-pass filtered M_{full} so it fluctuates less.

The modified gait pattern generates desired ground reaction force, F_{mdfd}, approximately equal to $F_{full} + F_{pend}$. Even if F_{full} is designed so that it satisfies the limits, there is no guarantee that the modified force F_{mdfd} does not exceed the limits.

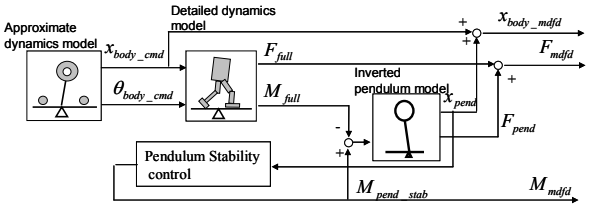

Fig. 4 Feedforward dynamics error compensation without ground reaction force limits

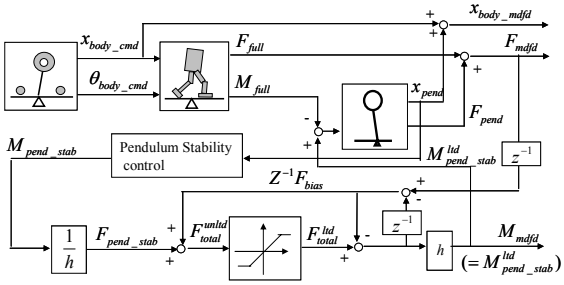

Fig. 5 Feedforward dynamics error compensation with ground reaction force limits in discrete time

B. Feedforward Dynamics Error Compensation with Ground Reaction Force Limits

Fig. 5 is the block diagram of the second compensation method, an extension from the first method to satisfy the ground reaction force limits.

According to Eq. (1)(2), if $M^{ltd}_{pend\_stab}(=M_{mdfd})$ is increased by $\Delta M^{ltd}_{pend\_stab}$, then F_{mdfd} increases by $\Delta M^{ltd}_{pend\_stab}/h$.

$$F_{mdfd} = M^{ltd}_{pend\_stab}/h + F_{bias} \tag{6}$$

where F_{bias} is the instantaneous value of F_{mdfd} when $M^{ltd}_{pend\_stab}$ becomes zero. Assuming that the value of F_{bias} did not change between the previous and current time steps, the expected value F^{unltd}_{total} of F_{mdfd} without limit in the current time step can be obtained as follows.

$$F^{unltd}_{total} = M_{pend\_stab}/h + Z^{-1}F_{bias} \tag{7}$$

where $Z^{-1}F_{bias}$ is the value of F_{bias} from the previous time step. F^{unltd}_{total} is input to the limiter in Fig. 5 which outputs a limited value, F^{ltd}_{total}, between $[F_{\min}, F_{\max}]$. Using the output from the limiter, the pendulum stabilizing moment $M^{ltd}_{pend\_stab}$ is determined.

$$M^{ltd}_{pend\_stab} = h(F^{ltd}_{total} - Z^{-1}F_{bias}) \tag{8}$$

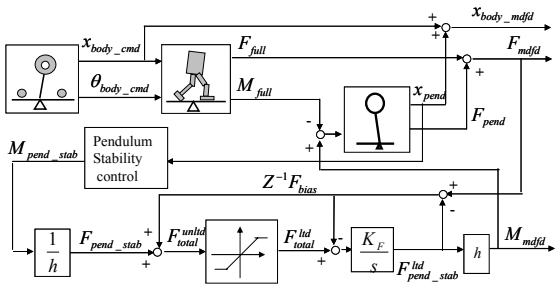

Fig. 6 Feedforward dynamics error compensation with ground reaction force limits in continuous time

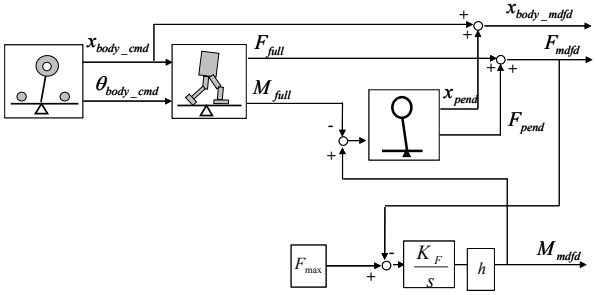

Fig. 7 Feedforward dynamics error compensation with ground reaction force limits for F_{total}^{unltd} exceeding $F_{\max}$

Note that $M_{pend\_stab}^{ltd}$ is the desired ground reaction moment of the compensated gait pattern.

Fig. 6 is the result of transforming Fig. 5 into continuous time domain. In case F_{total}^{unltd} exceeds $F_{\max}$, Fig. 6 transforms into Fig. 7 which ensures that F_{mdfd} follows $F_{\max}$ with integral feedback.

C. Feedforward Dynamics Error Compensation with Ground Reaction Force and Horizontal Moment Limits

Fig. 8 is the block diagram of the third compensation method which extends the second method to satisfy horizontal moment limits.

The limiter and distributor (shaded box in Fig. 8) takes M_{pend_stab}, M_{wheel_stab} and F_{mdfd} as inputs and outputs $M_{pend\_stab}^{ltd}$ and $M_{wheel\_stab}^{ltd}$. Using the outputs, the pendulum and the flywheel models are given following inputs.

$$M_{pend} = -M_{full} + M_{pend\_stab}^{ltd} \tag{9}$$

$$M_{wheel} = M_{wheel\_stab}^{ltd} \tag{10}$$

As shown in Fig. 8, the modified upper body motion which the real robot tries to follow is a sum of the trajectory designed with the approximate dynamics model, the pendulum motion and the flywheel motion. As a result, the desired ground reaction force is also a sum of the forces from the approximate dynamics model and the two compensation models.

$$F_{mdfd} = F_{full} + F_{pend} \tag{11}$$

$$M_{mdfd} = M_{full} + M_{pend} + M_{wheel} \tag{12}$$

From Eq. (9)(10)(12),

$$M_{mdfd} = M_{pend\_stab}^{ltd} + M_{wheel\_stab}^{ltd} \tag{13}$$

Note that F_{mdfd} is obtained from Eq. (6).

In case the ground reaction force and horizontal moment do not exceed the limits, the expected values of F_{mdfd} and M_{mdfd}, $(F_{total}^{unltd}, M_{total}^{unltd})$, can be computed as shown in Fig. 9. These values are input to the limiter which modifies them to F_{total}^{ltd} and M_{total}^{ltd} so that they do not violate admissible values. The details of how the limiter works are explained in the next section.

Note that $M_{pend\_stab}^{ltd}$ is computed in the same way as in the second method and $M_{wheel\_stab}^{ltd}$ is computed as follows.

$$M_{wheel\_stab}^{ltd} = M_{total}^{ltd} - M_{pend\_stab}^{ltd} \tag{14}$$

The modified gait pattern has admissible values of F_{mdfd} and M_{mdfd} by designing $M_{pend\_stab}^{ltd}$ and $M_{wheel\_stab}^{ltd}$ as explained above.

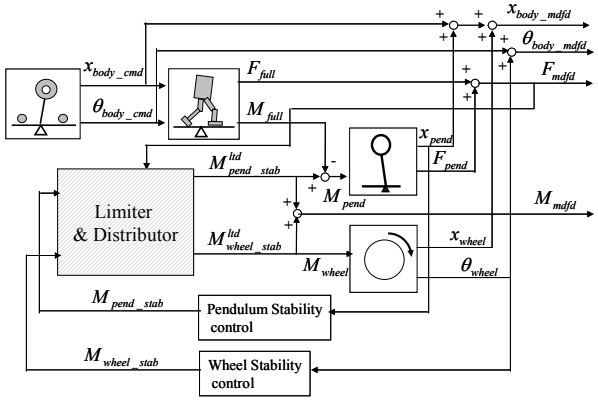

Fig. 8 Feedforward dynamics error compensation with ground reaction force and moment limits

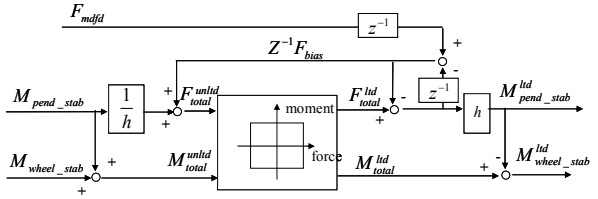

Fig. 9 Force and moment limiter and distributor

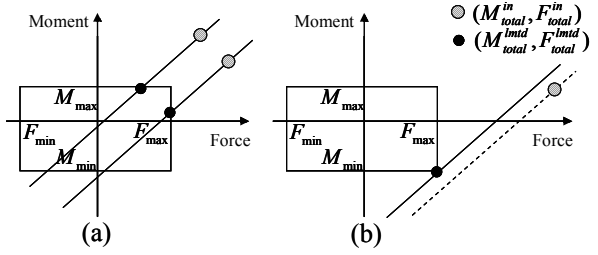

Fig. 10 Force and moment modification by the limiter

D. Ground Reaction Force and Momentum Limiter

The rectangle in Fig. 10 is the admissible range of the ground reaction force and moment. The limiter outputs the input $\left(F_{total}^{unltd}, M_{total}^{unltd}\right)$ without modification if its coordinate is inside this rectangle. On the other hand, if the point $\left(F_{total}^{unltd}, M_{total}^{unltd}\right)$ lies outside the triangle, $M_{wheel\_stab}^{ltd}$ is modified in such a way that $M_{wheel\_stab}^{ltd}$ becomes as close as possible to M_{wheel_stab}. Inputting moments which differs from M_{wheel_stab} by large amount causes the flywheel to diverge from its original state thus leading the upper body of the robot to incline largely. As shown in Fig. 10(a), a line which goes through $\left(F_{total}^{unltd}, M_{total}^{unltd}\right)$ and has inclination h is used to make the modification. Modification is made in such a way that Eq. (3) holds. As long as Eq. (3) is true, the motion can be realized by the inverted pendulum. Otherwise, the flywheel has to rotate to generate a moment which causes $M_{wheel\_stab}^{ltd}$ to diverge from M_{wheel_stab}.

In case the line goes through the rectangle, the intersection between the edge of the rectangle and the line which is closer to the original coordinate becomes the output. If the line does not intersect with the rectangle, the point on the edge of the rectangle which is closest to the line becomes the output.

The admissible values of F_{mdfd} are determined based on the friction between the ground and the sole of the feet and the admissible values of M_{mdfd} are determined so that the ZMP stays inside support polygon. Note that these admissible values are dependent on the vertical motion of the robot. During the flight phases when the vertical ground reaction force is 0, both M_{total}^{lmtd} and F_{total}^{lmtd} are 0.

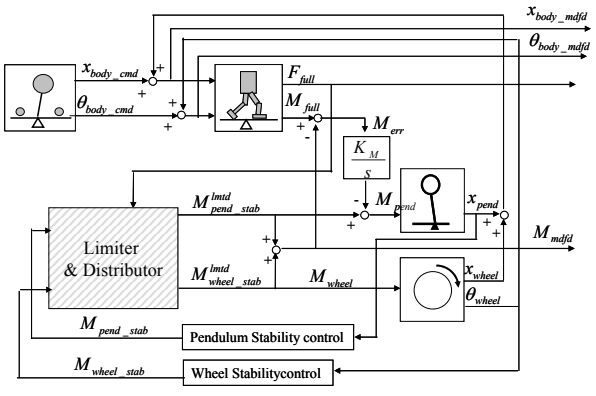

Fig. 11 Feedback dynamics error compensation

E. Feedback Dynamics Compensation

The previous section explained methods to modify gait patterns to compensate for the dynamics error between an approximate dynamics model and the detailed dynamics model using an inverted pendulum and a flywheel as dynamics compensation models. However, the integrated dynamics of the approximate dynamics model, inverted pendulum model and flywheel model do not strictly match that of the detailed dynamics model.

Fig. 11 is the block diagram for the FB method. The motions of dynamics error models, an inverted pendulum and a flywheel, are added to the original gait pattern and input to the detailed dynamics model. On the other hand, the motions of the dynamics error models in the FF methods are not input to the detailed dynamics models. The desired ground reaction moment of the modified gait pattern, M_{mdfd}, is set to $\left(M_{pend\_stab}^{ltd} + M_{wheel\_stab}^{ltd}\right)$.

M_{err}, the difference of M_{full} and $\left(M_{pend\_stab}^{ltd} + M_{wheel\_stab}^{ltd}\right)$ is integrated and input to an inverted pendulum model which has the same physical properties as the model used in the FF methods.

Compared to the FF method, the FB method is robust against the modeling error of the dynamics compensation models, the inverted pendulum and flywheel. However, the FF method has no delay in compensating the dynamics error while the FB method does.

From these properties of FF and FB methods, we serialize the two systems to achieve small delay and high accuracy. First the FF method eliminates large portion of the dynamics error without delay, and then the FB method prevents the remaining error from accumulating.

V. Knee Bending Dynamics Compensation

The approximate dynamics models we use to generate the original gait pattern do not have components corresponding to the knee bending motion of walking or running. This can cause large dynamics error especially for motions in which the knees of the robot bends quickly. Thus, we compensate for the knee motion using the following method and then feed the compensated motion into the FF and FB methods explained previously.

Fig. 12 shows the models we use to compensate for the knee bending dynamics. Fig. 12(a) is used to generate the original gait pattern, Fig. 12(c) is the detailed dynamics model of our real robot and the Fig. 12(b) is the telescopic model. The telescopic model has thigh, shin and upper body links. Each of the links has the same mass and inertia as those of the corresponding link of the detailed dynamics model. The CoG's of the thigh and shin links are located on the line which connects the hip joint and ankle joint.

Note that the GoG of the upper body link of the gait pattern designed with the approximate dynamics model is $x^s{}_b$ and the angle from vertical line is $\theta^s{}_b$. Also, the CoG of the thigh, shin and upper body links of the detailed dynamics model are

located at $x^c_{t[i]}$, $x^c_{s[i]}$ and x^c_b ([i] is either [R] or [L] for left and right leg respectively). The angles of each link are $\theta^c_{t[i]}$, $\theta^c_{s[i]}$ and θ^c_b. The masses are m_t, m_s and m_b, and the inertias are I_t, I_s and I_b. For the telescopic model, the CoG of the thigh, shin and upper body links of the telescopic model are located at $x^t_{t[i]}$, $x^t_{s[i]}$ and x^t_b ([i] is either [R] or [L] for left and right leg respectively). The angles of each link are $\theta^t_{t[i]}$, $\theta^t_{s[i]}$ and θ^t_b. The vertical CoG of each link are h^c_t, h^c_s and h^c_b respectively and assumed to be constant during motion. These values are determined from a standard upright posture of the robot in which the knees are bent at some angle. The position of the ankle joint of the detailed dynamics model and telescopic model are identical to that of the approximate dynamics model. Note also that x^t_b and θ^t_b are identical to x^s_b and θ^s_b respectively.

We solve the following two kinematic constraints iteratively for x^c_b and θ^c_b to compensate for the knee dynamics. x^c_b and θ^c_b are the modified upper body position and angle respectively.

$$m_b(x^c_b - x^t_b) + m_t\sum_i\left(x^c_{t[i]} - x^t_{t[i]}\right) + m_s\sum_i\left(x^c_{s[i]} - x^t_{s[i]}\right) = Const. \quad (15)$$

$$\begin{aligned} &m_b h^c_b \times (x^c_b - x^t_b) \\ &+ m_t\sum_i\left(h^c_{t[i]} \times (x^c_{t[i]} - x^t_{t[i]})\right) \\ &+ m_s\sum_i\left(h^c_{s[i]} \times (x^c_{s[i]} - x^t_{s[i]})\right) + I_b(\theta^c_b - \theta^t_b) \\ &+ I_t\sum_i\left(\theta^c_{t[i]} - \theta^t_{t[i]}\right) + I_s\sum_i\left(\theta^c_{s[i]} - \theta^t_{s[i]}\right) = Const. \end{aligned} \quad (16)$$

Regarding the difference of horizontal positions of each mass as velocity, Eq. (15) means that the total moment of the masses stays constant (Fig. 13(a)(b)). Eq. (16) refers to constant total angular momentum (Fig. 13(c)). From these kinematic computations, the dynamics error due to the knee bending motion is decreased.

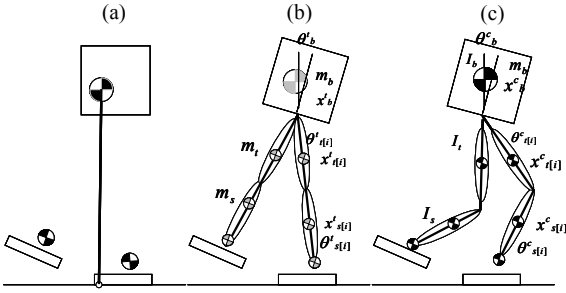

Fig. 12 Telescopic model and knee dynamics model

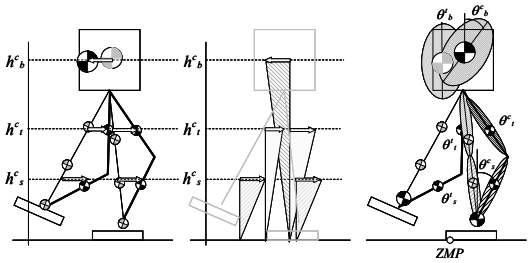

Fig. 13 Translational and rotational knee dynamics compensation

VI. RESULTS

We conducted experiments using a biped robot who is 130 cm tall. Each leg of the robot has 6 degrees of freedom. Fig. 14 is the moment generated about the desired ZMP trajectory transformed into equivalent ZMP error while walking at 4 km/h. As seen, the motion generated from the approximate dynamics error without compensation generates maximum error of 110 mm(A). With the knee dynamics compensation, the maximum error decreases to 90 mm(B). Furthermore, with the FF method following the knee dynamics error compensation and the FB method, the maximum error is less than 20 mm. The result confirms that proposed methods successfully compensates for dynamics error of the approximate dynamics model and realizes motion with large margin of stability.

Fig. 15 shows the behavior of the inverted pendulum and flywheel dynamics error compensation models with and without knee dynamics compensation while running at 6km/h. Without the knee dynamics compensation, both dynamics error compensation models diverge. With the knee dynamics, no divergence is observed. The result indicates effectiveness of the proposed knee dynamics error compensation technique. It also indicates that there is a limit on how much dynamics error the feedforward and feedback compensation techniques can compensate for as explained in previous sections.

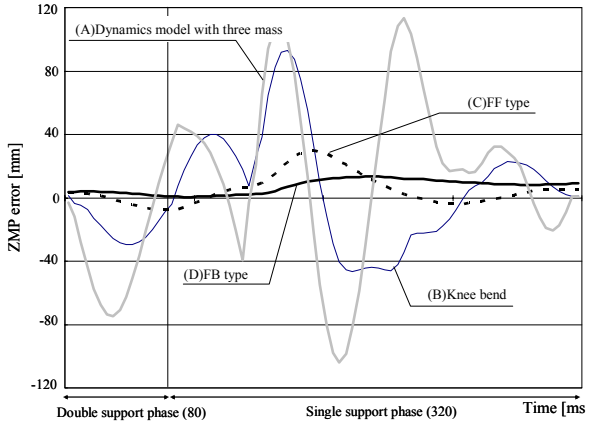

Fig. 14 ZMP error of 4km/h walking

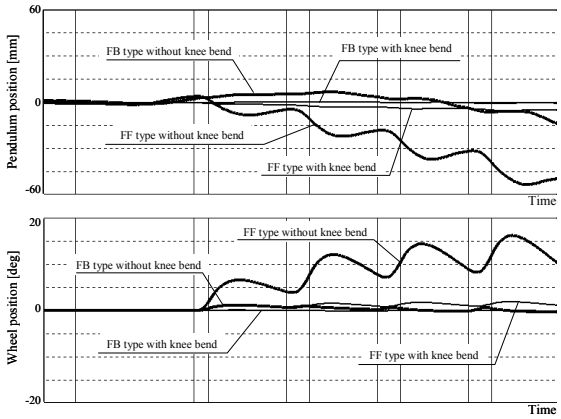

Fig. 15 Dynamics error model compensation for running at 6km/h

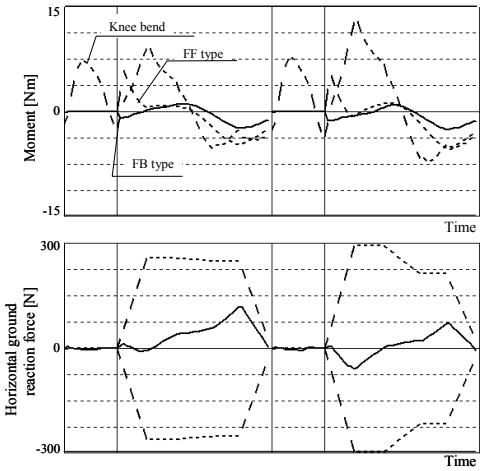

Fig. 16 Moment and horizontal ground reaction force of running at 6km/h

Fig. 16 shows the dynamics moment error and designed horizontal ground reaction force for running at 6 km/h expressed in the same unit as in Fig. 15. The three lines show dynamics error after the knee bending compensation, another followed by FF method, and another followed by FF and then FB methods. It can be observed that the ground reaction moment about the desired ZMP has decreased by the proposed compensation methods. Note that the ground reaction moment error is 0 (Fig. 16, top) and the designed horizontal ground reaction force (Fig. 16, bottom) is also 0 during the flight phase.

VII. CONCLUSIONS

In this paper, we proposed methods for correcting dynamics error of trajectories generated from approximate dynamics model of the real robot. The feedforward and feedback approaches using an inverted pendulum and a flywheel to approximate the dynamics error were proposed. The two methods keep the horizontal ground reaction force and moment under limits to prevent a slip between the foot and the ground. Another method to compensate for the motion of knees which our approximate dynamics model did not have is introduced. It was then shown that the knee dynamics compensation is an effective way to prevent the dynamics error compensation models of the feedforward and feedback approaches to diverge.

REFERENCES

[1] K. Hirai, M. Hirose, Y. Haikawa, and T. Takenaka, "The Development of Honda Humanoid Robot", In Proceedings of the 1998 IEEE International Conference on Robotics and Automation, Leuven, Belgium, May. 1998, pp. 1321-1326.

[2] Y. Sakagami, R. Watanabe, C. Aoyama, S. Matsunaga, N. Higaki, and K. Fujimura, "The intelligent ASIMO: System overview and integration", In Proceedings of the 2002 IEEE/RSJ International Conference on Intelligent Robots and Systems, 2002, pp. 2478-2483.

[3] S. Kajita, O. Matsumoto, and M. Saigo, "Real-time 3D Walking Pattern Generation for a Biped Robot with Telescopic Legs", In Proceedings of the 2001 IEEE International Conference on Robotics and Automation, 2001, pp. 2299-2306.

[4] T. Sugihara, Y. Nakamura, and H. Inoue, "Realtime Humanoid Motion Generation through ZMP Manipulation based on Inverted Pendulum Control", In Proceedings of the 2002 IEEE International Conference on Robotics and Automation, pp. 1404-1409, Washington DC, May, 2002.

[5] K. Nagasaka, Y. Kuroki, S. Suzuki, Y. Itoh, and J. Yamaguchi, "Integrated Motion Control for Walking, Jumping and Running on a Small Bipedal Entertainment Robot", In Proceedings of the 2004 IEEE International Conference on Robotics and Automation, New Orleans, 2004, pp. 3189-3194.

[6] K. Harada, S. Kajita, K. Kaneko, and H. Hirukawa, "An Analytical Method on Real-time Gait Planning for a Humanoid Robot", Journal of Humanoid Robotics, vol.3, no.1, pp.1-19, 2006.

[7] S. Kajita, F. Kanehiro, K. Kaneko, K. Fujiwara, K. Harada, K. Yokoi, and H. Hirukawa, "Biped Walking Pattern Generation by using Preview Control of Zero-Moment Point", In Proceedings of the 2003 IEEE International Conference on Robotics and Automation, 2003, pp. 1620-1626.

[8] K. Yamane and Y. Nakamura, "Dynamics Filter - Concept and Implementation of On-Line Motion Generator for Human Figures", IEEE Transactions on Robotics and Automation, vol. 19, no. 3, pp. 421-432, 2003.

[9] S. Kajita, F. Kanehiro, K. Kaneko, K. Fujiwara, K. Harada, K. Yokoi, and H. Hirukawa, "Resolved Momentum Control: Humanoid Motion Planning based on the Linear and Angular Momentum", In Proceedings of the 2003 IEEE/RSJ International Conference on Intelligent Robots and Systems, Oct. 2003, pp. 1644-1650.

[10] T. Takenaka, T. Matsumoto, and T. Yoshiike, "Real Time Motion Generation and Control for Biped Robot -1st Report: Walking Gait Pattern Generation-", In Proceedings of IEEE/RSJ International Conference on Intelligent Robots and Systems, 2009

[11] T. Takenaka, T. Matsumoto, T. Yoshiike, and S. Shirokura, "Real Time Motion Generation and Control for Biped Robot -2nd Report: Running Gait Pattern Generation-", In Proceedings of IEEE/RSJ International Conference on Intelligent Robots and Systems, 2009.

[12] T. Takenaka, T. Matsumoto, T. Yoshiike, T. Hasegawa, S. Shirokura, H. Kaneko, and A. Orita, "Real Time Motion Generation and Control for Biped Robot -4th Report: Integrated Balance Control-", In Proceedings of IEEE/RSJ International Conference on Intelligent Robots and Systems, 2009.

[13] K. Nagasaka, "The Whole Body Motion Generation of Humanoid Robot Using Dynamics Filter (in Japanese) ", Ph.D. dissertation, University of Tokyo, 2000

[14] J.Pratte, J.Carff, S.Drakunov and Ambarish Goswami, "Capture Point: A Step toward Humanoid Push Recovery", In Proceedings of the 2006 IEEE International Conference on Humanoids, 2006, pp. 200-207.